Chemical Science

ROYAL SOCIETY OF CHEMISTRY

EDGE ARTICLE

View Article Online
View Journal | View Issue

Cite this: *Chem. Sci.*, 2020, **11**, 2729

All publication charges for this article have been paid for by the Royal Society of Chemistry

Received 10th November 2019
Accepted 31st January 2020

DOI: 10.1039/c9sc05697a

rsc.li/chemical-science

Quinoline-containing diarylethenes: bridging between turn-on fluorescence, RGB switching and room temperature phosphorescence†

Zhen Xu, Qian T. Liu, Xiaozhu Wang, Qian Liu, Duane Hean, Keng C. Chou and Michael O. Wolf *

Simple structural modifications using oxidation and methylation of a quinoline-containing diarylethene result in dramatic variation of photophysical properties. Turn-on fluorescence, room temperature phosphorescence (RTP) and red-green-blue (RGB) switching were achieved in three different related compounds. Photoswitchable diarylethenes (DAEs) that exhibit turn-on fluorescence are in high demand for super-resolution microscopy, and the development of purely organic phosphorescent materials in the amorphous state is attractive but challenging. The findings reported here provide a novel toolkit for designing turn-on fluorescence DAEs for super-resolution microscopy and extending the scope of amorphous RTP materials. More importantly, we bridge between these two fundamentally significant photochemical and photophysical phenomena, and reveal structure–property relationships between DAE photochromism and RTP.

Introduction

Diarylethene compounds (DAEs), first introduced by Irie and co-workers, are a class of photochromic molecules which can undergo photocyclization and photocycloreversion between differently colored open and closed forms. They have been extensively studied over the last few decades due to their excellent thermal stability and photochromic fatigue resistance.[1–3] Many potential applications in optoelectronics such as optical recording and data storage, switchable catalysis as well as chemical and biological sensing have been envisioned.[3,4] These unique properties also position DAEs as excellent candidates as photo-switchable fluorophores for super-resolution fluorescence imaging. In this imaging technique, photoswitchable dyes with a highly emissive closed form (exhibiting turn-on fluorescence) are desirable as they give an initially dark background and enable off-on fluorescent switching. However, only a few examples of compounds that satisfy these criteria have been reported to date.[5–12] DAEs based on a 1,2-bis(2-ethyl-1-benzothiophene-1,1-dioxide)perfluorocyclopentene core have been used for super-resolution biological imaging and described as 'a universal tool for super-resolution microscopy in nanostructured materials'.[13–16] In order to further expand the scope of imaging dyes in both biology and materials science, new DAEs that exhibit turn-on fluorescence are in high demand.

In order to imbue DAEs with specific photophysical properties, it is common to functionalize them by appending chromophores to the thienyl units. For example, attaching tetraphenylethylene groups results in photo-switchable aggregation-induced emission while attaching a perylenemide chromophore allows fast fluorescence switching to be achieved.[17,18] However, this approach often requires numerous synthetic steps and typically does not fundamentally change the photochromic and photophysical properties of the DAEs, especially the fluorescent behavior of the closed form. It has been shown that replacing the perfluorocyclopentene ring in the DAE backbone with heterocycles can enrich the photochromic and photophysical behavior.[19,20] Even though extensive efforts have been made to enable fluorescence of the closed form, this is still a challenge and there remains a need to embed DAEs with novel photophysical behavior such as room temperature phosphorescence (RTP) in order to enrich the library of multi-functional photochromic compounds, gain a deeper understanding of photochemical and photophysical processes, and also to enable various applications in optoelectronics and bio-imaging.

The structure–property relationship between photochromic DAEs and room temperature phosphorescence (RTP) has not been studied. RTP has attracted great attention because it provides fundamental perspectives into metal-free triplet emission processes, and also inspires numerous potential applications in optoelectronics, as anti-counterfeiting inks, in addition to biological imaging.[21–25] To achieve organic RTP,

Department of Chemistry, University of British Columbia, 2036 Main Mall, Vancouver, BC, V6T 1Z1, Canada. E-mail: mwolf@chem.ubc.ca

† Electronic supplementary information (ESI) available: Experimental details and spectral data. See DOI: 10.1039/c9sc05697a

intersystem crossing (ISC) must be enhanced and molecular vibration and non-radiative decay supressed. Crystallization can help rigidify the molecular matrix in the solid state and provide stabilization for triplet excitons.[26–30] Even though this strategy has been extensively studied in recent years, there are still challenges involving processability (for light-emitting devices) and reproducibility due to crystal quality. It is therefore important to target new materials that display RTP in the amorphous state. Host–guest interactions, molecular assembly and polymerization have been utilized to achieve this goal,[31–38] however small molecules that show phosphorescence in the amorphous state have rarely been reported in the literature and most are highly halogenated.[8,39–42] To tackle these challenges, we decided to employ DAEs as building blocks for RTP materials. Not only does this provide new scope for molecular design of RTP materials, but it also enables the study of structure–property relationships between two well-known photochemical and photophysical phenomena: photochromism and RTP.

Herein, we report the synthesis, characterization, photochromic and luminescent properties of three closely related quinoline-containing diarylethenes (**1o**, **2o** and **3**) (Scheme 1). We chose a quinoline group for this purpose since not only does it result in the possibility of charge-transfer character in the DAE backbone but also provides an extra modification site at the nitrogen atom. Modification of the parent compound **1o** by oxidation of the thiophene sulfur atoms (**2o**) and methylation of the quinoline nitrogen (**3**) is achieved.

Results and discussion

Photoswitch **1o** was synthesized in 64% yield by Suzuki–Miyaura coupling between 3,4-dibromoisoquinoline and 2-methylbenzo[*b*]thiophene pinacol boronic ester. Oxidation of **1o** with *m*-CPBA in dichloromethane afforded photoswitch **2o** in 54% yield. Methylation of **1o** followed by anion exchange gave **3** in 84% yield. All compounds showed both parallel and anti-parallel conformations in the NMR spectra due to steric hindrance from the quinoline unit. For **1o** and **3** the conformers are present in a 1 : 1 ratio while **2o** exhibits a 2 : 1 ratio. Full synthetic and characterization details are available in the ESI.†

Compound **1o** exhibits characteristic diarylethene photocyclization behavior upon UV irradiation (365 nm) in dichloromethane (DCM) solution, changing from colorless to red and giving the closed form, **1c**. The broad absorption feature between 450–600 nm indicates formation of the more extended π-conjugated structure (Fig. 1a). The photostationary state is ∼28% **1c** as determined by NMR spectroscopy. Photocyclization and photocycloreversion quantum yields of **1o** are

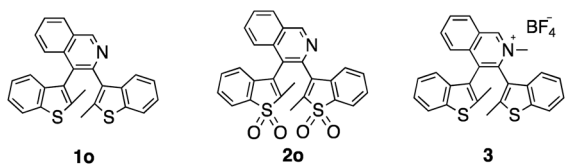

Scheme 1 Structures of quinoline-containing diarylethenes.

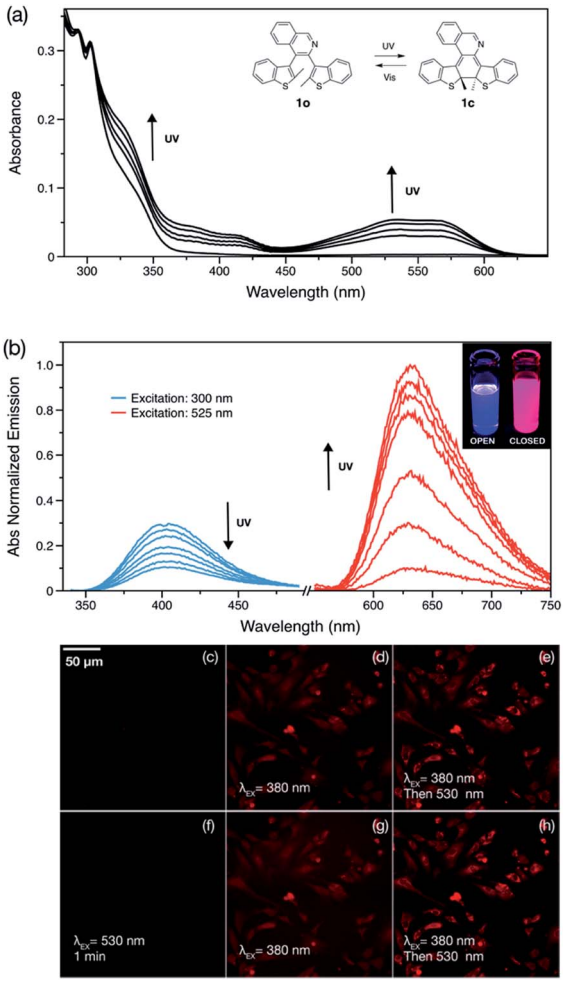

Fig. 1 (a) UV-vis spectral changes of **1o** (2.5×10^{-5} M) in dichloromethane upon UV irradiation. (b) Emission spectral changes of **1o** upon UV irradiation. (c–h):Sequence of fluorescence microscopy images of **1o** incubated HeLa cells (c) before irradiation, (d) after 30 s of 380 nm irradiation, (e) after brief 530 nm irradiation, (f) after 1 min 530 nm irradiation (g) after a second cycle of 30 sec 380 nm irradiation and (h) after brief 530 nm irradiation.

0.33 and 0.005, respectively (Table 1). Surprisingly, **1o** shows emission in both open and closed forms. The open form **1o** exhibits blue emission with a quantum yield of 0.04 in DCM solution while the closed form **1c** shows intense red emission with a quantum yield of 0.21 (Fig. 1b). There are only a handful of doubly emissive DAE compounds in the literature, and all examples show poor photoluminescence quantum yields (<0.02) in at least one of the two forms.[5,6,12] Incorporating a quinoline group into the DAE backbone opens a novel design strategy for doubly emissive DAE compounds.

To demonstrate the application of this compound as a dye for cellular imaging, HeLa cells were incubated with **1o**. The open form does not show any fluorescence initially under 530 nm excitation, however, once the cells are subjected to 380 nm irradiation from the fluorescence microscope, a red fluorescence appears which increases with time (Fig. 1d). Switching to 530 nm excitation gives stronger red emission at

Table 1 Photophysical and photochemical properties of **1** and **2** in DCM solution

		Open form			Closed form		
	PSS	λ_{max}/nm[a], (ε^b/10^4 M^{-1} cm^{-1})	$\Phi_F{}^c$	$\Phi_{O-C}{}^d$	λ_{max}/nm[a], (ε^b/10^4 M^{-1} cm^{-1})	$\Phi_F{}^c$	$\Phi_{C-O}{}^e$
1	0.28	305 (1.3)	0.04	0.22	530 (0.8), 575 (0.7)	0.21	0.005
2	0.34	315 (0.9), 330 (0.7)	N/A	0.14	430 (1.0), 455 (1.5), 488 (1.3)	0.55	0.13

[a] λ_{max}, absorption maximum. [b] ε, absorption coefficient. [c] Φ_F, fluorescence quantum yield. [d] Φ_{O-C}, cyclization quantum yield. [e] Φ_{C-O}, cycloreversion quantum yield.

first (Fig. 1e) and then the emission completely disappears in less than 1 minute (Fig. 1f). The fluorescence on–off cycles can be repeated several times (Fig. 1g and h show the beginning of the second cycle and Video S1†). The turn-on photochromic feature can be potentially used to improve the quality of the images but also to reduce false positive signals.[10,43]

The low photocycloreversion quantum yield and high brightness of the closed form make **1o** a suitable candidate for use in super-resolution imaging. The potential application of **1o** for this was tested with a home-built Single-Molecule Localization Microscope (SMLM).[44] A toluene solution of **1o** (nM concentration) was spin-coated onto a coverslip covered with fluorescent beads as fiducial markers. Previous studies revealed that diarylethenes can be activated using lasers with longer wavelengths due to the presence of Urbach tails, therefore, a single laser (532 nm) was used for activation, excitation and deactivation.[14,15,45–47] Compared to diffraction-limited fluorescent images (Fig. 2a), SMLM images are much clearer and provide more information regarding the local distribution of fluorophores (Fig. 2b). The decay profile of the number of photons collected from localized molecules of **1o** also shows good reversibility and stability (Fig. S4†). This proof-of-concept experiment confirms that the photochemical and photophysical properties of **1o** are suitable for super-resolution imaging.

Development of emissive compounds which can be switched between red, green and blue (RGB) emission is important for next-generation flexible full-color display technologies. However, it remains a challenge to develop a single component switching system which utilizes mild stimuli.[48–50] Due to the presence of the basic quinoline group, **1o** shows pH sensitivity in DCM solution. A solution of **1o** changes from colorless to pale yellow upon addition of trifluoroacetic acid (TFA) (Fig. 3a). Addition of acid results in a reduction in the intensity of the emission band of **1o**, while a new emission peak at 540 nm appears and increases in intensity; the new band is attributed to the protonated form **1-H$^+$** and has an emission quantum yield of 0.05 in DCM solution. This process is reversible by addition of trimethylamine, which deprotonates **1-H$^+$**. The different emission spectra of **1o**, **1c** and **1-H$^+$** enables tri-color switching using light and acid as stimuli. The protonated species **1-H$^+$** does not show any photoreactivity due to strong charge transfer from the thienyl units to the quinolinium group, thus no photoswitching from **1-H$^+$** to **1c** is observed.[4] Adding acid to a solution of **1c** quenches the red emission of this species. Tri-color switching thus requires the acid–base reaction to occur before irradiation with UV or visible light.

Oxidation of **1o** in DCM solution gave pale yellow **2o**. Unlike doubly emissive **1o**, the open form of **2o** shows no fluorescence. The closed form shows both well-structured absorption and emission in DCM solution (Fig. 4), indicative of the formation of a more rigid π-conjugated structure compared to **1c**. Oxidation of the benzo[*b*]thiophene causes a blue-shift of the emission and also results in an increase in Φ_F from 0.21 to 0.55 in the closed form, consistent with work by Irie.[8] The photostationary state contains 34% of the closed form.

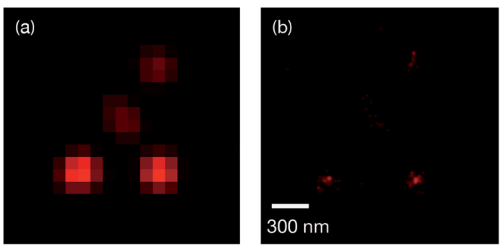

Fig. 2 (a) Diffraction-limited fluorescent image and (b) Super-resolution fluorescent image of **1o** in the solid state.

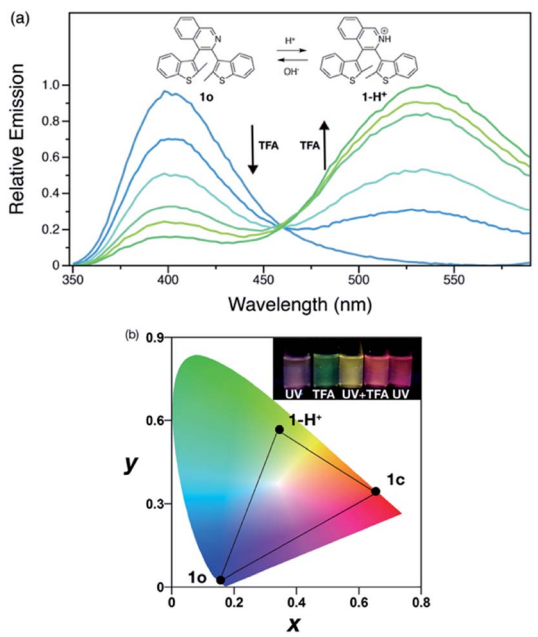

Fig. 3 (a) Emission spectral changes of **1o** (2.5×10^{-5} M) in DCM with TFA added. (b) Chromaticity plot of **1o**, **1c** and **1-H$^+$**. Inset: photos of **1o** under UV lamp with stimuli applied.

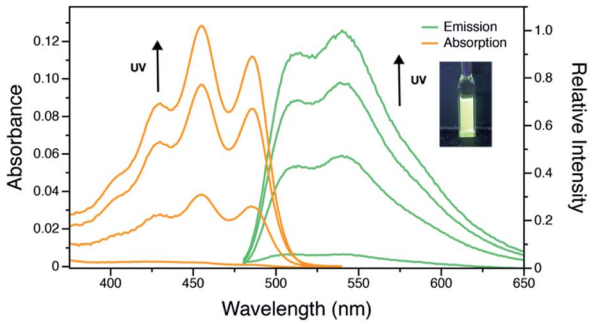

Fig. 4 UV-vis and emission spectral changes of **2o** (2.5×10^{-5} M) in DCM upon UV irradiation. Inset: photo of **2o** in the photostationary state under UV irradiation.

However, the photocyclization and photocycloreversion quantum yields of **2o** were found to be 0.14 and 0.13, respectively. The comparable photoreaction quantum yields make **2o** more suitable for optoelectronic applications in logic gates and chemical and biological sensing[43] rather than for super-resolution imaging. Compound **1o** also shows slightly better durability with multiple photoswitching cycles than **2o** (Fig. S12 and S13†).

Similar to **1-H$^+$**, the methylated compound **3** is also not photoreactive. This compound shows a bathochromic shift in different solvents with increasing polarity (Fig. 5a), indicative of a charge transfer state. The fluorescence quantum yield was found to be 0.07 in DCM solution and 0.09 in the solid state. Moreover, the charge transfer between benzo[*b*]thiophene units to the quinolinium group enhances ISC and opens up a pathway for RTP in the solid state. Computational studies suggest the HOMO and LUMO are well-separated spatially, which can facilitate intersystem crossing (Fig. S7†). As-prepared samples of **3** show very broad PXRD signals (Fig. 5b), indicating that this sample is likely amorphous. Surprisingly, the sample exhibits phosphorescence under ambient conditions. In steady-state studies, solid **3** exhibits green photoluminescence with a lifetime of 5 ns, however, a red-shifted component with an emission maximum of 575 nm was found when the prompt fluorescence is removed by collecting the spectrum with a 120 μs delay. The decay profile was monitored at 575 nm giving an average lifetime of 1.9 ms under ambient conditions, consistent with RTP. Variable temperature steady-state photoluminescence and phosphorescence lifetime measurements were also carried out (Fig. S2†). At 77 K, an emission maximum at 540 nm with a lifetime of 244 ms was observed, and a yellow 'afterglow' was observed by eye after the UV excitation was turned off (Video S2†). With increasing temperature, both the amplitude and lifetime of phosphorescence decreases. Due to instrumental limitations, time-resolved measurements were not accessible at low temperature. Nevertheless, these results confirm the observation of room temperature phosphorescence of **3** in what is most likely the amorphous state. We postulate that the cation–anion interactions between the DAE unit and $[BF_4]^-$ anion may both successfully isolate the emitter from oxygen and other triplet quenchers and reduce the vibrational dissipation of energy,[41] offering a novel and simple design principle for small molecule RTP in a non-crystalline state.

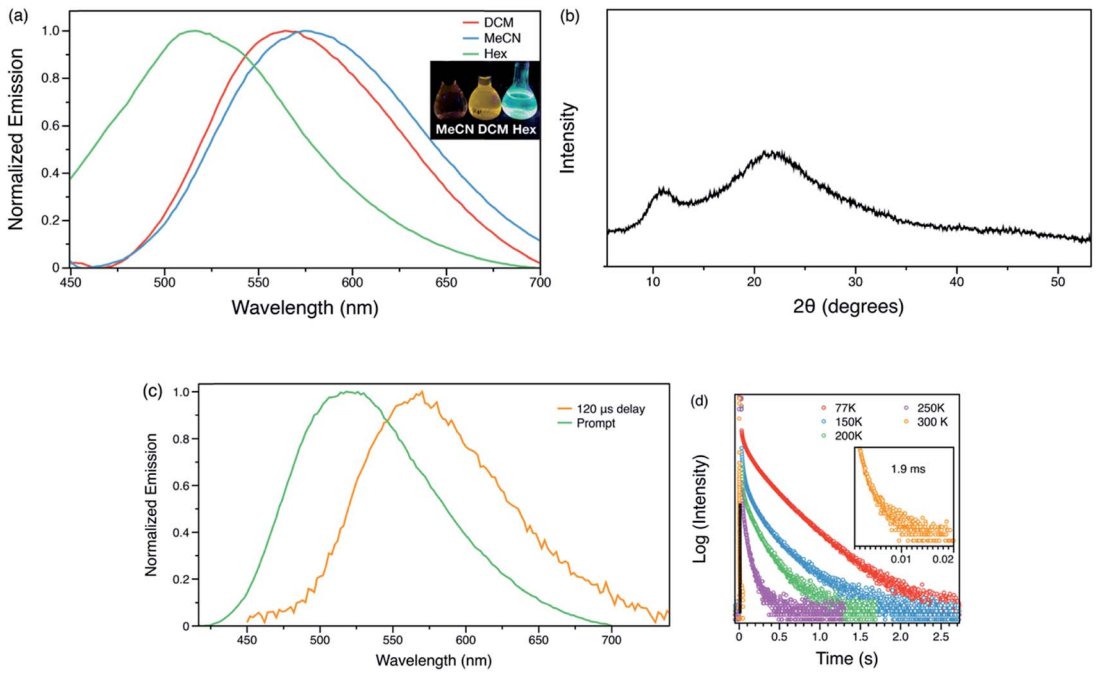

Fig. 5 (a) Emission spectrum of **3** (2.5×10^{-5} M) in hexanes (hex), DCM and acetonitrile (MeCN) solutions. (b) Powder XRD spectra of **3**. (c) Steady state and time-resolved emission spectra of **3** in amorphous state at ambient conditions. (d) Phosphorescence decay curves of **3** in the solid state at variable temperatures.

Conclusions

In summary, we present here a novel strategy to achieve multiple desirable photochemical and photophysical properties including RGB switching, turn-on fluorescence and room temperature phosphorescence (RTP) by simple structural modifications of a quinoline-DTE structure. Doubly emissive compound **1o** is demonstrated to be a potential fluorophore for super-resolution imaging and also presents a rare example of single component RGB switching, while oxidized product **2o** shows intense turn-on fluorescence, which can be potentially used for optoelectronic applications. Methylated **3** has strong charge transfer character that prevents photochromism but enables room-temperature phosphorescence. It also provides a rare example of small molecule RTP in a non-crystalline, likely amorphous state. These simple chemical modifications not only open the door to future molecular design for turn-on fluorescence and amorphous RTP, but also demonstrates the structure–property relationships between DAE photochromism and RTP.

Conflicts of interest

There are no conflicts to declare.

Acknowledgements

We acknowledge the Natural Sciences and Engineering Research Council of Canada for financial support and the Laboratory for Advanced Spectroscopy and Imaging Research (LASIR) for facilities access. We would like to thank Dr Saeid Kamal for assistance with the spectroscopic studies and Dr Christopher Brown for helpful discussions.

References

1 R. M. Kellogg, M. B. Groen and H. Wynberg, *J. Org. Chem.*, 1967, **32**, 3093–3100.
2 L. N. Lucas, J. van Esch, R. M. Kellogg and B. L. Feringa, *Chem. Commun.*, 1998, 2313–2314.
3 M. Irie, T. Fukaminato, K. Matsuda and S. Kobatake, *Chem. Rev.*, 2014, **114**, 12174–12277.
4 Z. Xu, Y. Cao, B. O. Patrick and M. O. Wolf, *Chem.–Eur. J.*, 2018, **24**, 10315–10319.
5 Y.-C. Jeong, S. I. Yang, K.-H. Ahn and E. Kim, *Chem. Commun.*, 2005, **408**, 2503–2505.
6 H.-H. Liu and Y. Chen, *J. Phys. Chem. A*, 2009, **113**, 5550–5553.
7 M. Taguchi, T. Nakagawa, T. Nakashima and T. Kawai, *J. Mater. Chem.*, 2011, **21**, 17425–17432.
8 K. Uno, H. Niikura, M. Morimoto, Y. Ishibashi, H. Miyasaka and M. Irie, *J. Am. Chem. Soc.*, 2011, **133**, 13558–13564.
9 Z. Li, J. Xia, J. Liang, J. Yuan, G. Jin, J. Yin, G.-A. Yu and S. H. Liu, *Dyes Pigm.*, 2011, **90**, 290–296.
10 S.-C. Pang, H. Hyun, S. Lee, D. Jang, M. J. Lee, S. H. Kang and K.-H. Ahn, *Chem. Commun.*, 2012, **48**, 3745–3747.
11 T. Sumi, T. Kaburagi, M. Morimoto, K. Une, H. Sotome, S. Ito, H. Miyasaka and M. Irie, *Org. Lett.*, 2015, **17**, 4802–4805.
12 T. Nakagawa, Y. Miyasaka and Y. Yokoyama, *Chem. Commun.*, 2018, **26**, 1827.
13 B. Roubinet, M. L. Bossi, P. Alt, M. Leutenegger, H. Shojaei, S. Schnorrenberg, S. Nizamov, M. Irie, V. N. Belov and S. W. Hell, *Angew. Chem., Int. Ed.*, 2016, **55**, 15429–15433.
14 B. Roubinet, M. Weber, H. Shojaei, M. Bates, M. L. Bossi, V. N. Belov, M. Irie and S. W. Hell, *J. Am. Chem. Soc.*, 2017, **139**, 6611–6620.
15 O. Nevskyi, D. Sysoiev, J. Dreier, S. C. Stein, A. Oppermann, F. Lemken, T. Janke, J. Enderlein, I. Testa, T. Huhn and D. Wöll, *Small*, 2018, **503**, 1703333.
16 Z. Qiang, K. M. Shebek, M. Irie and M. Wang, *ACS Macro Lett.*, 2018, **7**, 1432–1437.
17 C. Li, W.-L. Gong, Z. Hu, M. P. Aldred, G.-F. Zhang, T. Chen, Z.-L. Huang and M.-Q. Zhu, *RSC Adv.*, 2013, **3**, 8967–8972.
18 C. Li, H. Yan, L.-X. Zhao, G.-F. Zhang, Z. Hu, Z.-L. Huang and M.-Q. Zhu, *Nat. Commun.*, 2014, **5**, 5709.
19 J. C.-H. Chan, W. H. Lam and V. W.-W. Yam, *J. Am. Chem. Soc.*, 2014, **136**, 16994–16997.
20 N. M.-W. Wu, H.-L. Wong and V. W.-W. Yam, *Chem. Sci.*, 2017, **8**, 1309–1315.
21 Z. An, C. Zheng, Y. Tao, R. Chen, H. Shi, T. Chen, Z. Wang, H. Li, R. Deng, X. Liu and W. Huang, *Nat. Mater.*, 2015, **14**, 685–690.
22 Q. Li, Y. Tang, W. Hu and Z. Li, *Small*, 2018, **14**, 1801560.
23 H. Ma, Q. Peng, Z. An, W. Huang and Z. Shuai, *J. Am. Chem. Soc.*, 2018, **141**, 1010–1015.
24 J. Yang, X. Zhen, B. Wang, X. Gao, Z. Ren, J. Wang, Y. Xie, J. Li, Q. Peng, K. Pu and Z. Li, *Nat. Commun.*, 2018, **9**, 840.
25 Kenry, C. Chen and B. Liu, *Nat. Commun.*, 2019, **10**, 2111.
26 W. Z. Yuan, X. Y. Shen, H. Zhao, J. W. Y. Lam, L. Tang, P. Lu, C. Wang, Y. Liu, Z. Wang, Q. Zheng, J. Z. Sun, Y. Ma and B. Z. Tang, *J. Phys. Chem. C*, 2010, **114**, 6090–6099.
27 Z. Yang, Z. Mao, X. Zhang, D. Ou, Y. Mu, Y. Zhang, C. Zhao, S. Liu, Z. Chi, J. Xu, Y.-C. Wu, P.-Y. Lu, A. Lien and M. R. Bryce, *Angew. Chem., Int. Ed.*, 2016, **128**, 2221–2225.
28 Y. Gong, L. Zhao, Q. Peng, D. Fan, W. Z. Yuan, Y. Zhang and B. Z. Tang, *Chem. Sci.*, 2015, **6**, 4438–4444.
29 A. Forni, E. Lucenti, C. Botta and E. Cariati, *J. Mater. Chem. C*, 2018, **6**, 4603–4626.
30 Y. Xiong, Z. Zhao, W. Zhao, H. Ma, Q. Peng, Z. He, X. Zhang, Y. Chen, X. He, J. W. Y. Lam and B. Z. Tang, *Angew. Chem., Int. Ed.*, 2018, **57**, 7997–8001.
31 S. Hirata, K. Totani, J. Zhang, T. Yamashita, H. Kaji, S. R. Marder, T. Watanabe and C. Adachi, *Adv. Funct. Mater.*, 2013, **23**, 3386–3397.
32 S. Cai, H. Shi, Z. Zhang, X. Wang, H. Ma, N. Gan, Q. Wu, Z. Cheng, K. Ling, M. Gu, C. Ma, L. Gu, Z. An and W. Huang, *Angew. Chem., Int. Ed.*, 2018, **130**, 4069–4073.
33 D. Li, F. Lu, J. Wang, W. Hu, X.-M. Cao, X. Ma and H. Tian, *J. Am. Chem. Soc.*, 2018, **140**, 1916–1923.
34 L. Bian, H. Shi, X. Wang, K. Ling, H. Ma, M. Li, Z. Cheng, C. Ma, S. Cai, Q. Wu, N. Gan, X. Xu, Z. An and W. Huang, *J. Am. Chem. Soc.*, 2018, **140**, 10734–10739.

35 X. Ma, C. Xu, J. Wang and H. Tian, *Angew. Chem., Int. Ed.*, 2018, **130**, 11020–11024.
36 Z. Y. Zhang, Y. Chen and Y. Liu, *Angew. Chem., Int. Ed.*, 2019, **58**, 6028–6032.
37 X.-F. Wang, H. Xiao, P. Z. Chen, Q. Z. Yang, B. Chen, C. H. Tung, Y. Z. Chen and L.-Z. Wu, *J. Am. Chem. Soc.*, 2019, **141**, 5045–5050.
38 H. Wu, W. Chi, Z. Chen, G. Liu, L. Gu, A. K. Bindra, G. Yang, X. Liu and Y. Zhao, *Adv. Funct. Mater.*, 2019, **29**, 1807243.
39 J. Xu, A. Takai, Y. Kobayashi and M. Takeuchi, *Chem. Commun.*, 2013, **49**, 8447–8449.
40 B. Ventura, A. Bertocco, D. Braga, L. Catalano, S. d'Agostino, F. Grepioni and P. Taddei, *J. Phys. Chem. C*, 2014, **118**, 18646–18658.
41 W. Xu, Y. Yu, X. Ji, H. Zhao, J. Chen, Y. Fu, H. Cao, Q. He and J. Cheng, *Angew. Chem., Int. Ed.*, 2019, **58**, 16018–16022.
42 Z. He, H. Gao, S. Zhang, S. Zheng, Y. Wang, Z. Zhao, D. Ding, B. Yang, Y. Zhang and W. Z. Yuan, *Adv. Mater.*, 2019, **31**, 1807222.
43 T. Wu, B. Johnsen, Z. Qin, M. Morimoto, D. Baillie, M. Irie and N. R. Branda, *Nanoscale*, 2015, **7**, 11263–11266.
44 R. Tafteh, L. Abraham, D. Seo, H. Y. Lu, M. R. Gold and K. C. Chou, *Opt. Express*, 2016, **24**, 22959–22970.
45 Y. Arai, S. Ito, H. Fujita, Y. Yoneda, T. Kaji, S. Takei, R. Kashihara, M. Morimoto, M. Irie and H. Miyasaka, *Chem. Commun.*, 2017, **53**, 4066–4069.
46 R. Kashihara, M. Morimoto, S. Ito, H. Miyasaka and M. Irie, *J. Am. Chem. Soc.*, 2017, **139**, 16498–16501.
47 E. Siemes, O. Nevskyi, D. Sysoiev, S. K. Turnhoff, A. Oppermann, T. Huhn, W. Richtering and D. Wöll, *Angew. Chem., Int. Ed.*, 2018, **57**, 12280–12284.
48 J. E. Kwon, S. Park and S. Y. Park, *J. Am. Chem. Soc.*, 2013, **135**, 11239–11246.
49 L. Wang, K. Wang, H. Zhang, C. Jiao, B. Zou, K. Ye, H. Zhang and Y. Wang, *Chem. Commun.*, 2015, **51**, 7701–7704.
50 W. Li, Y.-M. Zhang, T. Zhang, W. Zhang, M. Li and S. X.-A. Zhang, *J. Mater. Chem. C*, 2016, **4**, 1527–1532.